Ultra-flat supercontinuum from 1.95 to 2.65 μm in a nanosecond pulsed Thulium-doped fiber laser

Clément Romano, Yves Jaouën, Robert E Tench, Jean-Marc Delavaux

Ultra-flat supercontinuum from 1.95 to 2.65 µm in a nanosecond pulsed Thulium-doped fiber laser

Clément Romano*[abc], Yves Jaouën[b], Robert E. Tench[a], Jean-Marc Delavaux[a]
[a]Cybel LLC, 1195 Pennsylvania Avenue, Bethlehem, PA USA 18018; [b]Télécom ParisTech, Institut Polytechnique de Paris, 46 Rue Barrault, 75634 Paris, France; [c]Fraunhofer IOSB, Gutleuthausstr. 1, 76275 Ettlingen, Germany
(At the time of this work, Clément Romano was with a & b, and is now with c)
*clement.romano@iosb.fraunhofer.de, www.cybel-llc.com

ABSTRACT

We report on mid-IR supercontinuum generation in an all-silica nanosecond pulsed fiber laser. The laser topology is a master oscillator power amplifier which consists of a two stage Thulium-doped fiber amplifier seeded with a directly modulated semiconductor laser at 1952 nm. The supercontinuum performance is investigated for repetition rate frequencies between 35 kHz to 100 kHz and pulse widths between 6 ns to 21 ns. Supercontinuum average output powers greater than 1.5 W and spectra ranging from 1.95 µm to 2.65 µm are demonstrated.

Keywords: Supercontinuum, pulsed, nanosecond, direct modulation, MOPA, Thulium, 2 microns.

1. INTRODUCTION

Supercontinuum sources are of great interest in the mid-IR region for medical, spectroscopy, and defense applications [1,2]. To be more specific, one extending from 1.95 to 2.65 um, could be used to detect seven gases which have absorption lines in this same region: NH_3, N_2O, CO, HF, C_2H_2, H_2S and NO [3,4,5]. To obtain a supercontinuum overlapping with this wavelength range, one can pump a highly nonlinear fiber. Usually, this fiber is a passive fiber with a small effective area and/or a high nonlinear material coefficient. One typical fiber with a high nonlinear material coefficient is the ZBLAN fiber ($n_2 \approx 2.4\text{x}10^{-17}$ $m^2.W^{-1}$, thousand times higher than silica fibers [6]), which allow transparency in middle IR (up to 4 µm). As an example, Heidt et al. pumped a ZBLAN fiber with a pulsed Thulium master oscillator power amplifier (MOPA) laser [7]. Although the resulting output ranges to even longer wavelength than 2.6 µm, it relies on a soft glass fiber, which handling or splicing is not as straight forward as a silica fiber [8].

An alternative white light source architecture, made out of pure silica fibers, for wavelength longer than 2 µm relies on a MOPA seeded by a 1.55 µm pulsed seed laser [9-12]. The MOPA is composed of multiple stages of Erbium-doped fiber amplifiers (EDFA) or Erbium:Ytterbium-doped fiber amplifiers (EYDFA) followed by at least one Thulium-doped fiber amplifier (TDFA). A supercontinuum ranging from 1.5 to 2.3 µm is initiated through the pulse amplification in the EDFAs and/or EYDFAs, and pulse breakup through non-linear processes in a few meters sample of single-mode fiber. The TDFA provides an amplification of this supercontinuum, suppress the wavelengths below 1.9 µm through absorption, and extend it to longer wavelength range (2 to 2.6 µm). Such architecture allows to have a flat supercontinuum over a range greater than 400 nm with high average power (> 5 W) [9-10,13] and a spectrum reaching long wavelength (> 2.6 um) [11-13].

Recently, thanks to the development of pulsed 2 µm lasers several supercontinuum sources, generating output performance with comparable spectrum and output power, have been demonstrated with a Thulium MOPA topology. The supercontinuum is directly generated inside the TDFA and in the output delivery silica fiber [14]. Generally, the generated supercontinuum extends from 1.8 µm to wavelengths longer than 2.5 µm [14-16] with average output powers greater than 10 W [16,17]. So far all the topologies reported use a seed laser which is based on a mode-locked (MD) or a gain-switched (GS) fiber laser cavity with pulse widths from femtoseconds [18] to nano-seconds. Here we demonstrate a simple supercontinuum source topology using a two stage TDFA seeded by a directly modulated (DM) laser diode. This structure is much simpler than the 1.5 µm seeded MOPA structure or the 2 µm seed MOPA structure with a mode-locked or gain-switched seed, and offers may new possibilities for practical devices.

2. EXPERIMENTAL TDFL SETUP

The supercontinuum (SC) source is based on the MOPA laser shown in Fig. 1. It is composed of a single-frequency seed laser, whose current is directly modulated, followed by a two stage TDFA. The seed is a semi-conductor laser operating at 1952 nm (Eblana Photonics). The two stage TDFA is a combination of a single-clad preamplifier and a double-clad booster amplifier.

In the CW regime, the seed laser delivers 2.6 mW at 1952 nm. In a pulsed regime, the combined bandwidth of the laser and the electronic driver allows us to generate pulse widths (defined at the full width half maximum (FWHM)) as short as 6 ns with pulse repetition frequencies (PRF) from kHz to MHz. With a pulse width of 21 ns, the seed laser delivers 85 μW for a PRF=2 MHz and only 0.4 μW for a PRF of 10 kHz. Such low seed laser average output power requires a careful amplifier design.

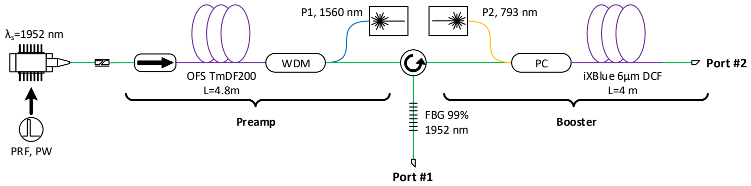

Fig. 1. Topology of our supercontinuum source.

The topology was chosen following multiple amplifier studies on single-clad and double-clad pumping in Thulium-doped fibers. Pumping a single-clad TDF with sources around 1560 has been demonstrated to provide high gain (> 35 dB) and low noise figure (close to the quantum limit) for low input powers (μW level) [19]. Such configuration relies on Er:Yb fiber laser pumps which for power scaling is not straight forward. Double-clad pumping a TDF using multimode diodes emitting around 793 nm was demonstrated to be efficient with an optical slope efficiency up to 74 % [20] and a path toward kW class MOPA laser [21].

The preamplifier is an improved design of a pulsed amplifier [22] based on a study [23] of slope efficiency comparison of single-clad fibers. It is based on a 4.8 m long Thulium-doped fiber (TDF), OFS TmDF200, counter-pumped by a 1560 nm fiber laser. The counter pumping topology was chosen because it provided a higher signal gain than the co-pumping configuration. A mid-stage 1 nm FBG (written on Nufern SM1950 fiber) filters the ASE from the preamplifier output to prevent saturation of the booster stage by the large ASE level from the preamplifier output. The design of the booster stage was found using a study on double-clad amplifiers [24]. The booster stage chosen topology is based on a co-pumped configuration, which compared to a counter-pumped configuration limits the length of output passive fiber. All the pumps (P1 & P2) of our Thulium-doped fiber laser (TDFL) were powered in a CW regime. All the components used in the setup are commercially available.

The performance of the laser was measured using the following equipment: a thermopile for the average output power, an optical spectrum analyzer (OSA, Yokogawa AQ6376) for the spectrum, and a high speed photodiode (12 GHz) for the pulse shapes. The output of the laser was attenuated before being launched into the OSA through a fiber jumper.

3. PRE-AMPLIFIER PERFORMANCE

We first studied the performance of a one stage laser composed of the semiconductor seed laser and the single-clad preamplifier. The wavelength laser seed was temperature tuned to 1951 nm in order to not match the FBG’s wavelength, which is centered at 1952 nm.

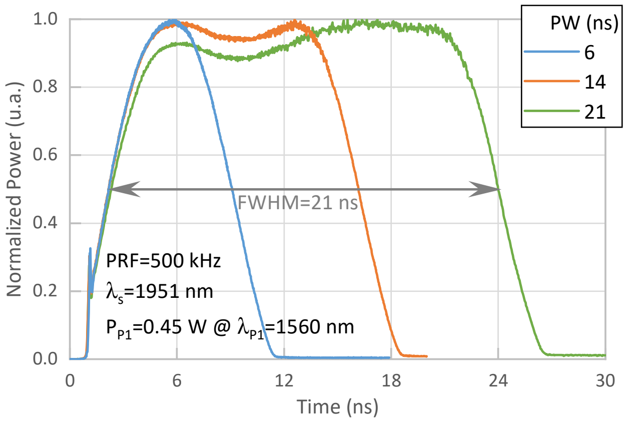

Fig. 2. Output pulse shape of the preamplifier for three different pulse widths.

The preamplifier pump power (P_{P1}) was set to 0.45 W during the whole study. We first investigated the normalized output pulse shape for three input pulse widths (PW), shown in Fig. 2 for a pulse repetition frequency of 500 kHz. No pulse distortion compared to the input pulse shape [22] was observed over all operating conditions for this pump power level.

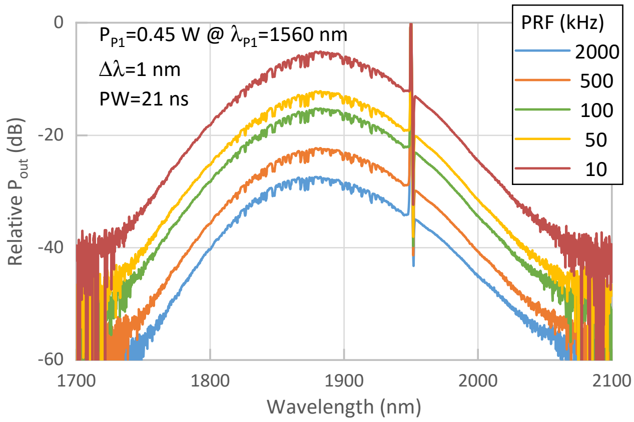

Fig. 3. Normalized output spectrum of the preamplifier for different pulse repetition frequencies and an input pulse width of 21 ns.

Figure 3 shows the normalized output spectrum of the preamplifier for a fixed 21 ns pulse width and a range of pulse repetition frequencies from 10 kHz to 2 MHz. The spectra were normalized to the peak of the spectrum, located at the signal wavelength. We noted that the total ASE power in the spectral bandwidth from 1700 to 2100 nm increased significantly as the PRF decreased. This observation meant that for low PRF values the amount of ASE is non negligible compared to the signal power and that an interstage ASE filter was necessary. Indeed, the presence of this mid-stage filter prevented the saturation of the booster stage by ASE power and yielded an increased optical-optical efficiency in the booster stage.

The calculated peak power (P_{peak}) versus PRF for three input pulse widths is plotted in Fig. 4. For all three input pulse widths tested, a maximum peak power of 11 W was reached for a PRF of 10 kHz, and decreased with increases in the PRF value. At a PRF of 2 MHz the peak power was 2, 4, and 5.5 W for pulse width of 21, 14, and 7 ns, respectively. With such high peak power values, the preamplifier output power (P_{out}) readily saturated the booster stage and efficiently extracted its optical energy.

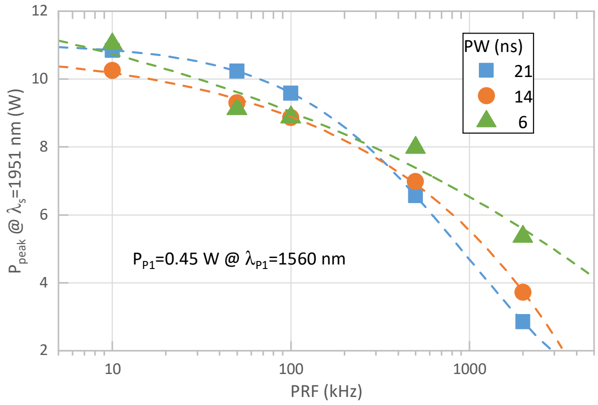

Fig. 4. Preamplifier output peak power versus pulse repetition frequencies for three input pulse widths.

4. SUPERCONTINUUM SOURCE PERFORMANCE

Next we evaluated the output performance of the two stage amplifier. The output power (Port #2 of the experimental setup) versus 793 nm pump power (P_{P2}) is shown in Fig. 5 for PRFs from 35 kHz to 100 kHz at a seed pulse width of 6 ns. The slope efficiency (η) is defined as the variation of output power divided by the variation in pump power. We observed that the slope efficiency above threshold was not constant with the pump power. Indeed, the slope efficiency followed a two step process; for each PRF the output power first increased with a 46 % slope efficiency and then switches to a lower 8 % slope efficiency. The slope efficiency decrease corresponded to the spectral broadening of the seed laser by non-linear effects generating a supercontinuum output. We noted that this change of slope efficiency was observed independently of the PRF but this effect was a function of the PRF. Operation of the booster stage power was limited by the onset of lasing at the peak of the ASE around 2000 nm.

The output spectrum of our laser was then recorded for different operating pump powers P2 and these spectra are plotted in Fig. 6 for a PRF of 100 kHz. We observed that for a low pump power of 1.2 W (blue line), only the signal and the ASE centered around 2000 nm were present. At a higher pump power of 2.1 W (orange line), the output spectrum exhibited important side lobes on each side of the signal. For pump powers of 3.6 W and higher, we observed a supercontinuum spread from 1950 nm to wavelengths as high as 2700 nm, which is the highest wavelength usually observed in silica fibers. As the pump increased, the signal at 1952 nm decreased gradually and while an increase at longer wavelengths occurred. The absorption lines in the SC spectrum around 2600 nm were not the result of the active or passive fiber used in our topology. Water present in air absorbs from 2.6 to 2.8 µm [3]. Our OSA was not purged with a neutral gas and so measuring these absorption lines was possible.

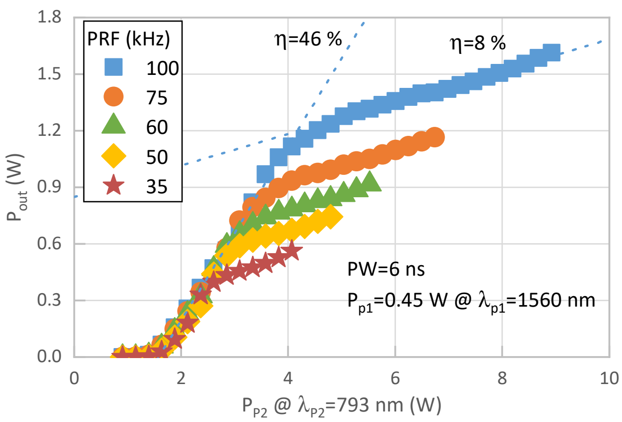

Fig. 5. TDFL output power versus 793 nm pump power for different PRFs.

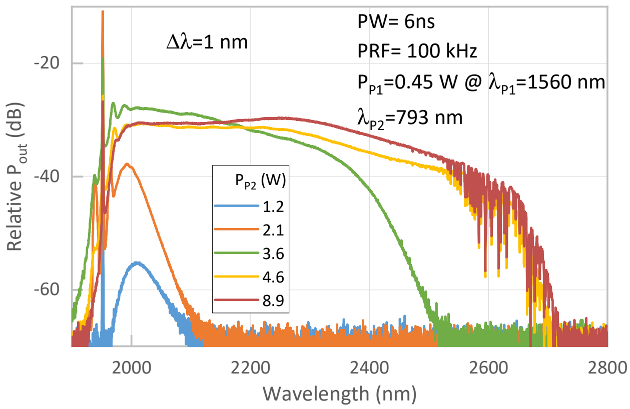

Fig. 6. Output spectrum for different 793 nm pump power level.

We define the bandwidth (BD) of this supercontinuum using a 10 dB criterion below the spectrum peak value, regardless of the residual peak at the signal wavelength of 1952 nm. The PRF of the seed laser was then varied and we studied the bandwidth of the SC as a function of the pump power in Fig. 7. We observed, independently of the PRF, the same evolution of the SC spectrum: first we witnessed a linear increase of the supercontinuum BD with pump power, followed then by a plateau. We observed that for PRF of 50 kHz and above the SC bandwidth can be as large as 600 nm.

Figure 8 shows the maximum output power measured dominated by a supercontinuum versus the PRF for pulse widths of 6, 14, and 21 ns. This plot revealed that: 1) for a fixed PRF value change of pulse widths did not produce large difference in average SC P_{out}, 2) smaller pulse width values yielded larger SC power levels, and 3) the SC power increased linearly with increases in PRF, as it has already demonstrated in other supercontinuum sources [1,25]. A maximum SC average P_{out} of 1.6 W was measured and may have scaled with higher pump power.

For our initial spectral measurements of the SC shown in orange in Fig. 9, the signal was attenuated and coupled to the OSA through a fiber jumper (Nufern SM1950, L=2.5 m). During our measurements our assumption was that such a jumper, with even a short length, could induce distortion of the measured SC spectrum. So in order to verify our point, the output of the SC source was free space coupled to the OSA and measured again (in blue in Fig. 9). Both SC spectra with (orange line) and without (blue line) the fiber jumper revealed a strong difference for wavelength from 2250 nm and higher. The measurement made with the jumper clearly exhibited the silica background losses. The 10 dB bandwidth of the SC measured without the fiber jumper was 690 nm instead of the 600 nm with the jumper fiber in place.

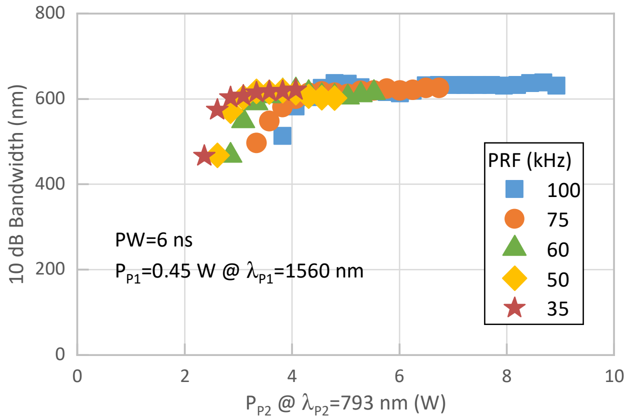

Fig. 7. Supercontinuum 10 dB bandwidth versus 793 nm pump power for different pulse repetition frequencies.

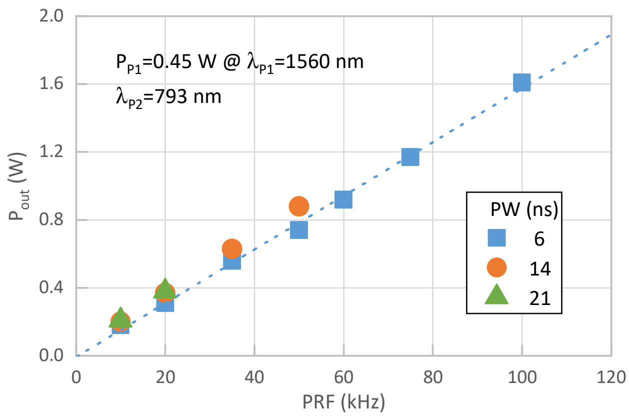

Fig. 8. Supercontinuum average output power versus pulse repetition frequency for three seed pulse widths.

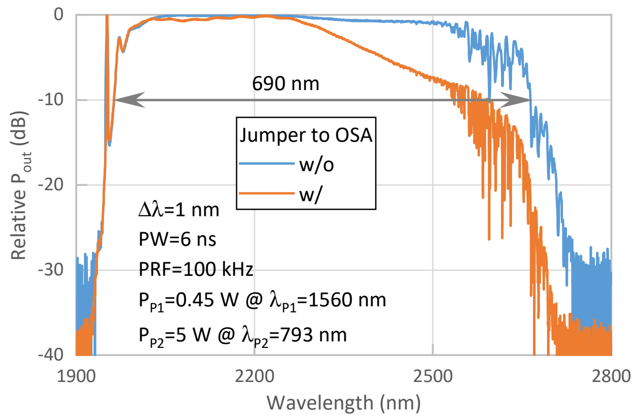

Fig. 9. Comparison of measured spectra coupled differently into the OSA.

Finally, we studied the output power stability of the SC source. The output power was set to 1.3 W and monitored over 6 hours. The power evolution over this period is shown in Fig. 10. We measured a peak to peak stability less than 4 % over a period of 6 hours. The active fiber of the booster was held on an aluminum plate with no active heat sinking. As the supercontinuum is generated in the active fiber and the efficiency drops, the heat released increases. The heat management is believed to be the cause of the output power variation.

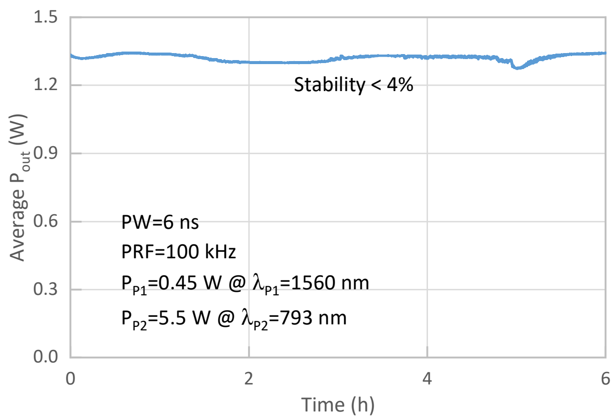

Fig. 10. Output power stability over a 6 hour period.

5. DISCUSSION

As the dispersion of Thulium-doped fibers has been measured to be in the anomalous regime ($D \approx 9$ $ps.km^{-1}.nm^{-1}$ @ 2000 nm [26]) it is indeed prone to modulation instability with high peak powers, which ignite the supercontinuum [1]. We first compare our results with the ones reported so far. Table 1 contrasts some of the most important results published on MOPA all-silica supercontinuum sources using a 2 µm pulsed seed source. We would like to point that most of these SC sources are based on amplifying a ML laser, a specific design that can be somewhat difficult to assemble and reproduce. One exception is Yao et al.'s paper [27] that relies on a commercial GS diode. In comparison to all these SC sources, our simple and rugged SC source design offers the widest bandwidth, with 690 nm at 10 dB, combined with a readily scalable output power.

Ref	PRF (kHz)	AVG P_{out} (W)	BD (nm)	Seed source
[5]	100	2.8	610	GS / ML
[14]	14 000	1.7	450	ML
[15]	3 000	70	550	ML
[16]	334 000	36	450	ML
[17]	56 000	0.7	250	ML
[28]	77 000	6.8	550	ML
[27]	40 000	142	615	GS
[29]	29 390	62.1	634	ML
[30]	93 600	42	> 460	ML
This work	100	1.6	690	DM

Table 1. Literature review of 2 µm seeded MOPA all-silica supercontinuum sources.

Still, we believe that the performance of source can be further improved. Based on our measurements shown in Fig. 8, the use of shorter pulse modulation (i.e. < 6 ns) and higher pump powers should lead to higher SC average output powers [11,25]. For example, the use of 1 ns pulse width will also allow the use of larger PRF (i.e. > 100 kHz) as shown by Fig. 8. It has been shown that the passive and active fiber length are important for the generation of the supercontinuum [14,26], and it would be interesting to study the SC generation as a function of the passive and active fiber length in order to optimize the SC performance. In addition, such a study would allow us to decrease the contribution of the pulsed seed laser in the output SC spectrum.

As we have illustrated earlier the choice and length of the passive fiber can degrade or deliver the true bandwidth available. A fiber with a transmission bandwidth capable of transmitting the full spectrum would make our SC MOPA design even more practical: a hollow-core single-mode fiber may be a possible solution.

Another way to improve the performance of the non-linear conversion (slope efficiency and threshold) would be to use a counter-pumped booster configuration, as shown by Dvoyrin and Sorokina [28]. On the other hand, for the same SC output power the same authors observed a decrease of the bandwidth from > 550 nm in a co-pumped configuration to 440 nm in a counter-pumped configuration.

The decrease of the slope efficiency with the pump power increasing illustrated in Fig. 5 has already been measured in a similar supercontinuum configuration [16]. The change of slope efficiency can be explained through the high signal loss seen for long wavelengths (i.e. ≈1 dB/m @ 2.3 µm [15]) and so is inherent to the configuration type. Clearly the spectral BD of our supercontinuum source will always be limited by the intrinsic losses of silica but are still subject to improvement. The only way to reach longer wavelengths is to use other materials or doping. As an example, it has been demonstrated that using a pulsed MOPA laser combined with an output pigtail of germanate fiber (silica fiber highly doped in GeO_2) the generated supercontinuum can reach wavelengths longer than 3 µm [31]. This can be achieved because these types of fibers have their background losses shifted toward longer wavelengths and like the all-silica fibers they are in the anomalous regime ($D > 0$ $ps.nm^{-1}.km^{-1}$) around 2 µm [31]. Still such fibers offer the advantage of being "easy" to splice to other silica doped fibers, and they do not have to rely on mechanical splices like fluoride fibers.

6. CONCLUSION

We have investigated a supercontinuum laser source with a spectrum extending from 1.95 to 2.65 µm with a maximum output power of 1.6 W at a repetition rate frequency of 100 kHz and a 6 ns pulse width. This source was designed around a simple and reliable two stage MOPA configuration where the seed laser current was directly modulated with ns pulses. First, we investigated the performance of a one stage MOPA laser, which delivered multi watt peak power in the nanosecond regime. Next, we have demonstrated that the addition of a double-clad fiber stage booster could scale the output power to produce a multi watts SC source. This SC source performance was fully characterized as a function of pulse width and pulse repetition frequency.

7. ACKNOWLEDGEMENTS

We thank iXblue for the double-clad TDF, OFS for the single-clad TDF, Eblana Photonics for the single-frequency semiconductor laser source at 1952 nm and Mr. Brad Sicotte from Teracomm for lending us the OSA.

8. BIBLIOGRAPHY

[1] Alexander V.V., et al., "Modulation instability initiated high power all-fiber supercontinuum lasers and their applications," Opt. Fiber Technol. **18**(5), 349-374 (2012).

[2] Labruyère A., et al., "Compact supercontinuum sources and their biomedical applications," Opt. Fiber Technol. **18**(5), 375–378 (2012).

[3] HITRAN Database, https://hitran.org/

[4] Jahromi K. E., et al., "Mid-infrared supercontinuum-based upconversion detection for trace gas sensing," Opt. Express, **27**(17), 24469, (2019).

[5] Yin K., et al., "Ultrahigh-brightness, spectrally-flat, short-wave infrared supercontinuum source for long-range atmospheric applications," Opt. Express **24**(18), 20010 (2016).

[6] Agrawal G. P., "Nonlinear fiber optics," Chapter 11, (2013).

[7] Heidt A. M., et al., "High Power Diode-Seeded Fiber Amplifiers at 2 µm-From Architectures to Applications," IEEE Journal of Selected Topics in Quantum Electronics **20**(5), 525–536, (2014).

[8] Yin K., et al. "Highly stable, monolithic, single-mode mid-infrared supercontinuum source based on low-loss fusion spliced silica and fluoride fibers," Opt. Lett. **41**(5), 946 (2016).

[9] Alexander V. V., et al., "Power scalable >25 W supercontinuum laser from 2 to 25 µm with near-diffraction-limited beam and low output variability," Opt. Lett. **38**(13), 2292 (2013).

[10] Yin K. et al., "Over 100 W ultra-flat broadband short-wave infrared supercontinuum generation in a thulium-doped fiber amplifier," Opt. Lett. **40**(20), 4787 (2015).

[11] Swiderski J., and Michalska M., "Mid-infrared supercontinuum generation in a single-mode thulium-doped fiber amplifier," Laser Physics Lett. 10(035105) (2013).

[12] Xue G., et al., "Stable high-spectral-flatness mid-infrared supercontinuum generation in Tm-doped fiber amplifier," Opt. Fiber Technol. 24, 1–4 (2015).

[13] Yin K., et al., "Ultrahigh-brightness, spectrally-flat, short-wave infrared supercontinuum source for long-range atmospheric applications", Opt. Express **24**(18), 20010 (2016).

[14] Tao M., et al., "Super-flat supercontinuum generation from a Tm-doped fiber amplifier," Sci. Rep. **6**, 23759 (2016).

[15] Xing S., et al., "Generation of high-brightness spectrally flat supercontinuum in 1900–2450 nm range inside a small core thulium-doped fiber amplifier," Proc. OSA ASSL, AM5A.8 (2016)

[16] Ouyang D., et al., "Mid-infrared Spectral Intensity Enhanced Supercontinuum Generation Based on Nanosecond Thulium-Doped Fiber Laser," IEEE Photonics J. **8**(3), 1600910 (2016).

[17] Liu J., et al., "High average power picosecond pulse and supercontinuum generation from a thulium-doped, all-fiber amplifier," Opt. Lett. **38**(20), 4150–4153 (2013).

[18] Luo J., et al., "Mid-IR supercontinuum pumped by femtosecond pulses from thulium doped all-fiber amplifier," Opt. Express. **24**(13), 13939-13945 (2016).

[19] Li Z., et al., "Thulium-doped fiber amplifier for optical communications at 2 µm," Opt. Express, **21**(8), 9289–9297, (2013).

[20] Ehrenreich T., et al., "1-kW , All-Glass Tm:fiber Laser," Proc. SPIE Fiber Lasers III: Technology, Systems, and Applications, 7580-112 (2010).

[21] Petit V., et al., “Highly doped and highly efficient Tm doped fiber laser,” Proc. SPIE Fiber Lasers XV: Technology and Systems, 105120M (2018).
[22] Romano C., et al., “kW pulsed nanosecond TDFL with direct modulation,” Proc. SPIE Fiber Lasers XVI: Technology and Systems, 1089708 (2019).
[23] Romano C., et al., “5 W 1952 nm Brillouin-free efficient single clad TDFA,” Opt. Fiber Technol. **46**, 186–191 (2018).
[24] Romano C., et al., “Simulation and design of a multistage 10W thulium-doped double clad silica fiber amplifier at 2050nm,” Proc. SPIE Fiber Lasers XIV: Technology and Systems, 100830H (2017).
[25] Swiderski J., and Michalska M., “Mid-infrared supercontinuum generation in a single-mode thulium-doped fiber amplifier,” Laser Physics Lett. **10**, 035105 (2013).
[26] Kharitonov S., et al., “Kerr nonlinearity and dispersion characterization of core-pumped thulium-doped fiber at 2 μm,” Optics Letters, **41**(14), 3173 (2016).
[27] Yao W., et al., “Gain-switched laser diode seeded TDFA with 409 W picosecond pulses and 142 W spectrally flat supercontinuum output,” Opt. Express, **27**(2), 1276-1282 (2019).
[28] Dvoyrin V. V., and Sorokina I.T., “6.8 W all-fiber supercontinuum source at 1.9–2.5 μm,” Laser Phys. Lett. **11**(8), 085108 (2014).
[29] Yang W., et al., “Thirteen watt all-fiber mid-infrared supercontinuum generation in a single mode ZBLAN fiber pumped by a 2 μm MOPA system,” Opt. Lett. **39**(7), 1849 (2014).
[30] Liu K., et al., “High power mid-infrared supercontinuum generation in a single-mode ZBLAN fiber with up to 21.8 W average output power,” Opt. Express **22**(20), 24384 (2014).
[31] Jain D., et al., “Scaling power, bandwidth, and efficiency of mid-infrared supercontinuum source based on a GeO2-doped silica fiber,” J. Opt. Soc. Am. B. **36**(2), A86-A92 (2019).